

# Protonolysis of Fe-C bonds of a Diiminopyridineiron(II) Dialkyl Complex by Acids of Different Strengths: Influence of Monoanionic Ligands on the Spectroscopic Properties of Diiminopyridine-FeY<sub>2</sub> Complexes.

M. Ángeles Cartes, Pilar Palma, John J. Sandoval, Juan Cámpora\* and Eleuterio Álvarez.

*Instituto de Investigaciones Químicas, CSIC – Universidad de Sevilla. c/ Américo Vespucio, 49, 41092, Sevilla, Spain.*

## Summary

The reaction of the dialkyliron complex  $[\text{Fe}(\text{CH}_2\text{SiMe}_3)_2(\text{MesBIP})]$  (MesBIP = 2,6-bis((*N*-mesityl)acetimidoyl)pyridine) with protic acids (HY) of different strengths ( $\text{Y} = \text{C}_6\text{F}_5\text{O}, \text{CF}_3\text{CO}_2, \text{Cl}, \text{CF}_3\text{SO}_3$ ) invariably leads to the cleavage of both Fe-C bonds, independently of the Fe/HY ratio used (either 1:2 or 1:1), affording the corresponding complexes  $[\text{FeY}_2(\text{MesBIP})]$ . Relevant spectroscopic features of these compounds, such as paramagnetic <sup>1</sup>H NMR shifts and UV-VIS absorption bands, exhibit a marked dependence on the nature of Y.

*Keywords: 2,6-bisiminopyridine ligands, iron, alkyl complexes, olefin polymerization.*

## 1. Introduction

Olefin polymerization or oligomerization catalysts based on iron complexes of 2,6-bisiminopyridine (BIP) ligands have attracted much interest due to their high activity and the abundance and low toxicity and of iron.<sup>[1]</sup> In addition, the modular design of BIP ligands facilitates the variation of the stereoelectronic environment of the active centre, enabling a precise control of the molecular weight of the polymers. It is usually assumed that, similarly to other polymerization systems, activation of  $[\text{FeX}_2(\text{BIP})]$  complexes with alumoxanes or other organoaluminum-based co-catalysts give rise to catalytically active alkyliron species. Such a classic Ziegler-Natta mechanism gained strong support in 2005, when Chirik prepared cationic complexes of the type  $[\text{Fe}(\text{R})(\text{S})(\text{iPrBIP})]^+$  (iPrBIP = BIP ligand with 2,6-diisopropylphenyl as aryl substituent in the imine; S = OEt<sub>2</sub>, THF, or none) by protonation of dialkyl precursors with  $[\text{HNPhMe}_2]^+ [\text{BPh}_4]^-$ ,<sup>[2]</sup> and demonstrated that such cationic iron alkyls behave as highly active single-component catalysts for ethylene polymerization. However, the precise nature of the active species on the real catalysts generated with the aid of alkylaluminum co-catalysts is still the subject of some controversy. The latter are known to play a very important role in the catalytic process, influencing both the activity and the molecular

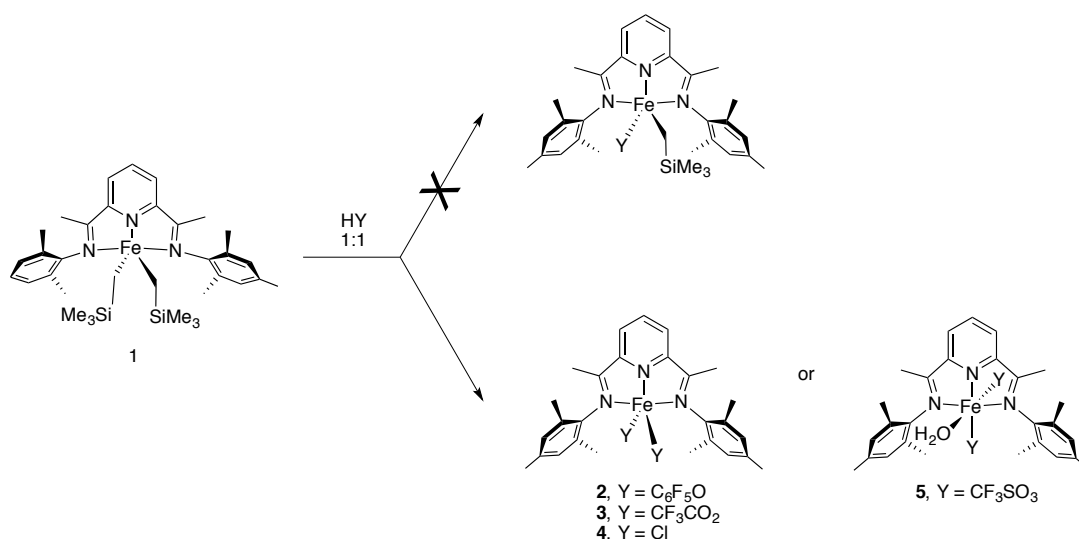
---

\* E-mail address: [campora@iq.csic.es](mailto:campora@iq.csic.es) (J. Cámpora).

weight distribution of the polyolefinic products.<sup>[3]</sup> Indeed, spectroscopic investigations of the aluminium-activated iron catalysts by Bryliakov and Talsi have revealed that the interaction of  $[\text{FeX}_2(\text{BIP})]$  complexes with organoaluminum reagents gives rise to both neutral and cationic bimetallic Fe/Al species that very likely have an active participation in the polymerization process.<sup>[4]</sup> In addition, it has been recognized that the counteranion that balances the electric charge of active cationic species plays a role of crucial importance in the performance of most homogeneous Ziegler-Natta polymerization catalysts.<sup>[5]</sup> Thus, it seems very likely that iron complexes of the type  $[\text{Fe}(\text{R})(\text{Y})(\text{BIP})]$  (where Y symbolizes an anionic ligand) should exhibit significant differences in their ability to act as polymerization catalysts, as the coordinating strength of Y or its ability to interact with the co-catalysts can be varied widely. Several years ago, we reported a general methodology that provides access to iron dialkyl complexes of the type  $[\text{Fe}(\text{CH}_2\text{SiMe}_3)_2(\text{BIP})]$ ,<sup>[6]</sup> and we wondered whether these complexes could react selectively with protic acids HY of different strengths to afford the desired  $[\text{Fe}(\text{CH}_2\text{SiMe}_3)(\text{Y})(\text{BIP})]$  complexes. As we show in this contribution, it turned out that such mixed ligand compounds are not stable or cannot be produced through this route. Instead, the protonation reaction affords symmetrical  $[\text{FeY}_2(\text{BIP})]$  derivatives. This allowed us to compare some of the key spectroscopic features of these compounds and analyse how these properties are influenced by the nature of the anionic Y ligand.

## 2. Results and Discussion.

We investigated the reactions of the readily available dialkyl complex  $[\text{Fe}(\text{CH}_2\text{SiMe}_3)_2(\text{MesBIP})]$  (**1**) with four protic acids of different strengths: Pentafluorophenol ( $\text{pK}_a = 5.4$ ), trifluoroacetic acid ( $\text{pK}_a = 0.2$ ), hydrogen chloride ( $\text{pK}_a = -7$ ) and triflic acid ( $\text{pK}_a = -12$ ).<sup>[7,8]</sup> Stoichiometric (1:1) amounts of the acids diluted in THF were slowly added to the solutions of the iron dialkyl in the same solvent at  $-80\text{ }^\circ\text{C}$ , and then allowed to slowly warm to room temperature. In spite of the care taken to control the reaction conditions, these reactions invariably led to products **2 – 5** resulting from the cleavage of both Fe-C bonds of **1** (Scheme 1). The products were precipitated by addition of hexane, leaving purple mother liquors containing unreacted **1**. As expected, higher yields of all four products were obtained when the acids and the iron alkyl were reacted in 2:1 ratio. These results suggest that the non-symmetrical alkyl complexes  $[\text{Fe}(\text{CH}_2\text{SiMe}_3)(\text{Y})(\text{MesBIP})]$  are unstable and rapidly disproportionate in solution affording a mixture of the corresponding symmetrical complexes. This conclusion is also supported by Chirik's observation that the reaction of the mixed complex  $[\text{Fe}(\text{CH}_2\text{SiMe}_3)(\text{Cl})(\text{Py})_2]$  with  ${}^{\text{iPr}}\text{BIP}$  does not afford the intended (chloro)trimethylsilylmethyl derivative  $[\text{Fe}(\text{CH}_2\text{SiMe}_3)_2(\text{Cl})({}^{\text{iPr}}\text{BIP})]$ , but a mixture of the dialkyl and dichloro complexes.<sup>[9]</sup>



Scheme 1

Apart from the well-known chloro derivative **4**,<sup>[3]</sup> none of the rest of the products, **2**, **3** and **5**, has been described previously. They are all paramagnetic with  $\mu_{\text{eff}} = 5.0 - 5.6 \mu_{\text{B}}$  at room temperature, consistent with a high-spin configuration with four unpaired electrons. Crystals of **2** and **5** suitable for X-ray analysis were obtained by recrystallization. Figures 1 and 2 show ORTEP views of these two complexes, and Table 1 collects selected bond lengths and angles. Remarkably, very few iron bisimino pyridine complexes containing alkoxy or aryloxy ligands have been reported before,<sup>[10]</sup> and to the best of our knowledge, no dialkoxy or diaryloxy derivatives have been reported before. Similarly to the analogous halide complexes [FeX<sub>2</sub>(<sup>Me<sup>s</sup></sup>BIP)] (X = Cl, Br), the iron centre of the aryloxy **2** exhibits a distorted trigonal bipyramidal geometry, with the imine nitrogen atoms occupying the axial positions. The  $\tau$  parameter,<sup>[11]</sup> that describes the distortion degree between perfect bipyramidal trigonal ( $\tau = 1$ ) and square pyramidal ( $\tau = 0$ ) geometries, takes the value 0.84 for this compound. A crystallographically imposed mirror plane bisects the molecule through the iron and the three nitrogen atoms and relates the pentafluoroaryloxy moieties. The latter are oriented in such a way that one of the *ortho* fluorine substituents (F5) approaches to the iron atom. This conformation could be favoured by an attractive electrostatic interaction, but the Fe-F5 distance (3.0149(12) Å) is too long to mean any significant chemical bonding. As it is usually found in this type of compounds, the Fe-N bonds involving the imino groups are somewhat different, decreasing the overall molecular symmetry from C<sub>2v</sub> (if both Fe-imine bonds were identical) to C<sub>s</sub>. The structure of complex **5** contains, in addition to the triflate ligands, a molecule of water attached to the iron centre. The presence of an aqua ligand is also revealed by a strong absorption at 3345 cm<sup>-1</sup> in the IR spectrum of this compound. Very likely, this water comes from adventitious traces of moisture in the solvents during the synthesis or the recrystallization of this complex, and its presence reveals the strong Lewis acidity of the corresponding bis-triflate precursor. Britovsek has reported related

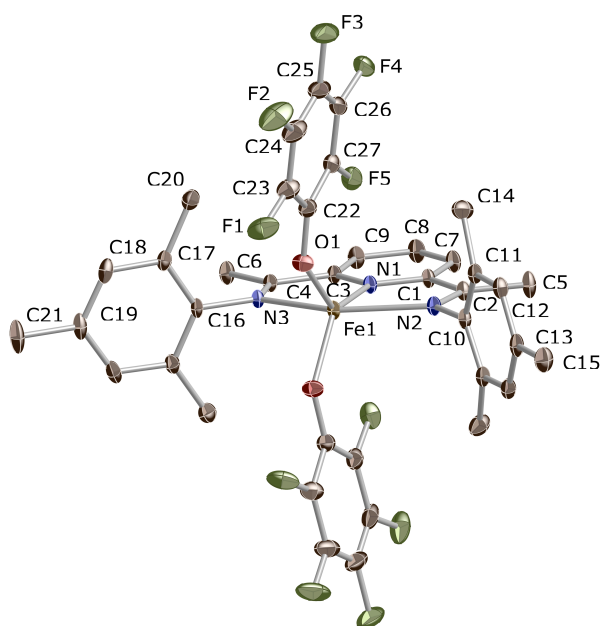


Figure 1. ORTEP view of the X ray structure of compound **2**

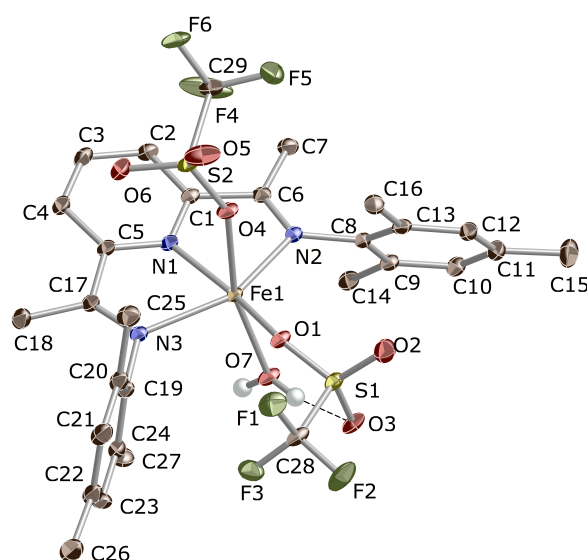


Figure 2. ORTEP view of the X ray structure of compound **5**.

Table 1: Selected bond distances (Å) and bond angles (°) for compounds **2** and **5**.

Distances (Å)	<b>2</b>	<b>5</b>	Angles (deg)	<b>2</b>	<b>5</b>
Fe-N1	2.0943(17)	2.089(2)	O1-Fe-O1'/O4	97.06(7)	84.32(7)
Fe-N2	2.2923(17)	2.236(2)	N1-Fe-N3	73.97(6)	74.50(8)
Fe-N3	2.2368(17)	2.210(2)	N2-Fe-N3	147.58(6)	147.71(8)
Fe-O1	1.9840(11)	2.1084(18)	O1-Fe-N1	131.36(3)	62.26(7)
Fe-O4	--	2.2277(19)	O4-Fe-N1	--	93.82(7)
Fe-O7	--	2.1288(18)	O7-Fe-N1	--	110.88(8)
O7... <i>(H)</i> ...O3	--	2.804(3)	O1-Fe-N2	103.14(5)	118.47(7)
			O1-Fe-N3	98.14(5)	93.82(7)

Fe(II) and Mn(II) bis-triflate complexes with BIP ligands. Interestingly, the Mn(II) derivative containing the <sup>Me</sup><sub>2</sub>BIP ligand (*N*-aryl groups = 2,6-dimethylphenyl) was also isolated as the monohydrate [Mn(OTf)<sub>2</sub>(OH<sub>2</sub>)(<sup>Me</sup><sub>2</sub>BIP)].<sup>[12]</sup> Goldberg has recently reported a mixed iron(II) thiolate-triflate complex. [Fe(OTf)(SPh)(<sup>i</sup>PrBIP)].<sup>[13]</sup> The geometry of the iron centre in **5** is approximately octahedral, with the aqua ligand and one of the triflate ligands occupying “axial” positions, i. e., perpendicular to the main coordination plane defined by the three N atoms of the BIP ligand and the second triflate group. This configuration contrasts with that preferred by the analogous manganese complex [Mn(OTf)<sub>2</sub>(OH<sub>2</sub>)(<sup>Me</sup><sub>2</sub>BIP)], which shows both triflate groups in the axis and the aqua ligand sharing the equatorial plane with the BIP ligand.<sup>[9]</sup> A hydrogen bond links the aqua ligand of **5** to the *cis* triflate group. The distance between the oxygen atoms

involved in this interaction, O3 and O7, (2.804(3) Å) suggests that the H bridge is relatively weak, as it is longer than those observed in typical O...H...O hydrogen bonds, for instance those formed in water or in carboxylic acids (2.6 – 2.7 Å).<sup>[14]</sup> The Fe-O bonds (either those involving the triflate or aqua ligands) are 2.1 – 2.2 Å long, significantly longer than the Fe-O bonds in the aryloxide **2** (1.9840(11) Å). This difference is due in part to the higher coordination number in **5**, but they also reflect the weaker nature of the Fe-O bonds involving the aqua and triflate anions, the latter predominantly ionic in character. Although we were unable to grow X-ray quality crystals of carboxylate **3**, this compound probably has a pentacoordinated structure with terminally bound carboxylate ligands, as observed for related carboxylate compounds containing terpy<sup>[15]</sup> or related tridentate N,N,N ligands.<sup>[16]</sup> Terminal coordination of the trifluoroacetate ligands is supported by the large separation between the IR absorptions for the  $\nu_s$  and  $\nu_{as}$  modes of the carboxylate group, observed at 1697 and 1260  $\text{cm}^{-1}$  ( $\Delta\nu = 437 \text{ cm}^{-1}$ ).<sup>[17]</sup>

The colours of complexes **1** – **5** are strikingly varied. While the dialkyl **1** is purple, perfluorophenolate **2** is green, the trifluoroacetate and triflate derivatives **3** and **5** are burgundy-red and magenta, respectively, and the chloro complex **4** is dark blue. The origin of these colours is a broad absorption band in the visible spectrum, whose position varies depending on the anionic ligands coordinated to the iron centre (Figure 3). The absorption maximum ( $\lambda_{\text{max}}$ ) appears at 550 nm for **1** and shifts to longer wavelengths for the products arising from the protonation with acid, in the order **1** < **2** (580 nm) < **3** (625 nm) < **4** (680 nm). This band has also been observed in the visible spectra of other iron-BIP complexes and assigned to a charge transfer transition involving the BIP ligand.<sup>[18]</sup> The observed trend indicates that the energy gap between the orbitals responsible for the transition decreases as the acid HY from which the complex arises becomes stronger, or what is the same, as the anion  $\text{Y}^-$  becomes more electronegative. This points to a ligand to metal (LMCT) rather than a metal to ligand charge transfer band (MLCT), since electron withdrawing from the metal is expected to lower the energy of metal-centred orbitals, while leaving those of the BIP ligand relatively unaffected. Triflate complex **5** is the exception to the mentioned trend, as its visible absorption occurs at 550 nm, when it would be expected to be the lowest in energy for the series. This apparent exception is readily explained by the presence of the additional aqua ligand, which contributes to compensate the electronic deficiency caused by the strongly electron-withdrawing triflate ligands on the metal centre.

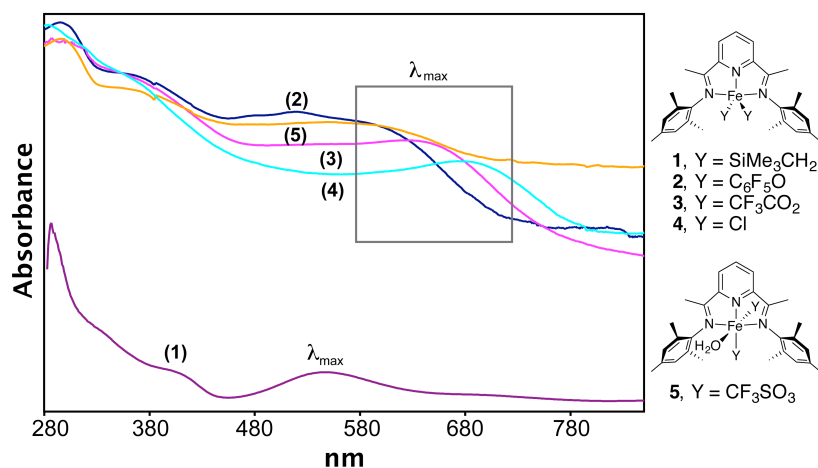


Figure 3. UV-VIS spectra of complexes **1** – **5**.

High spin Fe(II) complexes with BIP ligands give rise to useful NMR spectra. Typically, the  $^1\text{H}$  signals have linewidths between a few and several hundred hertz and can be readily observed, except those belonging to groups directly attached to the metal centre. These signals can be assigned on the basis of their intensity, width and their characteristically large chemical shifts. Recognizing trends in the spectra of series of related complexes is highly helpful in the task of assigning resonances, and constitutes a useful tool for the identification of new complexes. The  $^1\text{H}$  NMR spectra of complexes **2** – **5** provide some of such useful trends (see Figure 4). Since none of the ligands Y contain H atoms, these spectra show only signals corresponding to the  $^{\text{Mes}}$ BIP ligand. They all exhibit the same number of signals, corresponding to apparent  $\text{C}_{2v}$  molecular symmetry. In the case of the triflate complex, the simplicity of the spectrum is not consistent with the lower symmetry observed in the solid state, indicating that in solution the aquo and triflate ligands exchange their relative positions, probably *via* a mechanism involving OTf dissociation. This is supported by the  $^{19}\text{F}$  spectrum, which shows a single resonance at  $\delta$  -14.6 ppm in dichloromethane, which shifts to -71.0 ppm in acetonitrile, close to the position expected for an uncoordinated triflate anion.<sup>[12]</sup> One of the most evident features of these spectra is the strong sensitivity of the chemical shift of some of the  $^{\text{Mes}}$ BIP signals to the nature of ligands Y. The signal H4 is particularly noteworthy, as it shifts to higher field in the order Y = Cl (complex **4**, 34.8 ppm)  $\approx$   $\text{C}_6\text{F}_5\text{O}$  (**2**, 35.5 ppm) > triflate (**5**, 22.7 ppm) > trifluoroacetate (**3**, -11.2 ppm). The signal for the  $\alpha$ -methyl of the imino group shows the same tendency, but with the opposite sign: **2** (-22.6 ppm)  $\approx$  **4** (-22.2) < **5** (-3.6 ppm) < **3** (+4.1 ppm). The inverse correlation between the chemical shifts of the H4 and  $\alpha$ -Me signals holds for the dialkyl **1**, for which they take extreme values, +284.0 and -184.3, respectively. The analogous signals in other Fe(II) dialkyl complexes containing BIP ligands exhibit similar extreme paramagnetic shifts.<sup>[6,9,10]</sup> The observed H4/ $\alpha$ -Me sequences bear no simple relationship with the

donor capacity of Y, since paramagnetic chemical shifts depend on the spin density on the observed nucleus rather than on partial electric charge effects. However, the much larger paramagnetic shifts of the position of H4 and  $\alpha$ -Me signals in **1** enables us to discriminate between simple coordination complexes containing mild  $\sigma$ -donor Y groups from organometallic species.

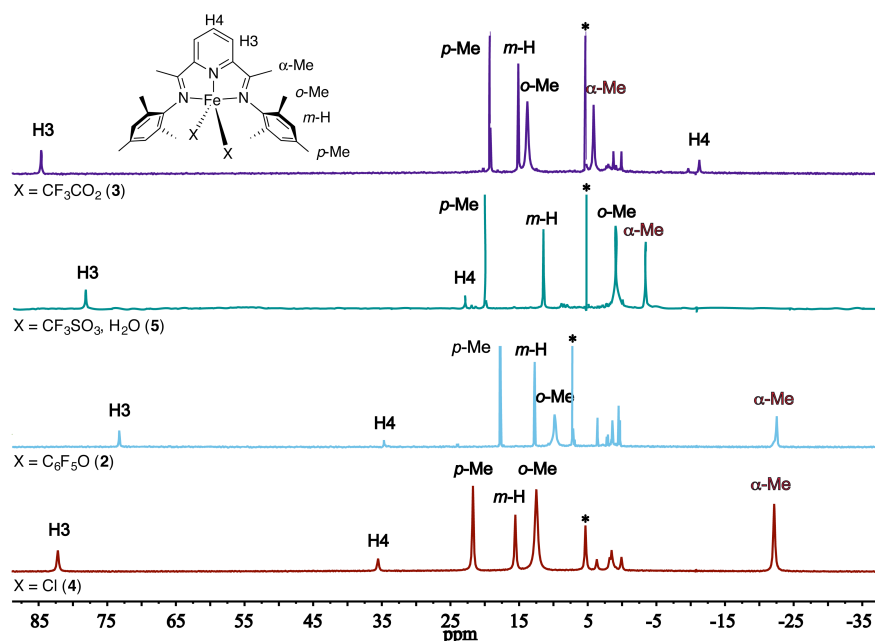


Figure 4.  $^1\text{H}$  NMR spectra of complexes **2**–**5**. Residual peaks of deuterated solvent ( $\text{C}_6\text{D}_6$  for **2** and  $\text{CD}_2\text{Cl}_2$  for **3**, **4** and **5**) are marked with asterisk (\*).

### 3. Conclusions

Our attempts to selectively cleave one Fe-C bonds of the dialkyl **1** with a variety of protic acids HY of different strengths have been unsuccessful, as these reactions invariably lead to  $[\text{FeY}_2(\text{MesBIP})]$  complexes arising from the cleavage of both Fe-C bonds. We evaluated the influence of ligands Y on the spectroscopic properties of this series of complexes. The charge transfer absorption band responsible for the colour of these complexes shifts to longer wavelengths as the electron density on the Fe atom, controlled by the Y ligands, decreases. Although the chemical shift of some  $^1\text{H}$  NMR signals of the  $^{\text{Mes}}\text{BIP}$  ligand (in particular, those due to pyridine H4 and the imine  $\alpha$ -Me group) are very sensitive to the nature of Y, no clear-cut relationship is observed. These exhibit much larger paramagnetic shifts in the organometallic parent compound **1** than in the coordination complexes **2**–**5**.

## 4. Experimental Section

*4.1. General considerations.* All manipulations were carried out under inert atmosphere by using conventional Schlenk techniques or a nitrogen-filled glovebox. Solvents were rigorously dried and degassed prior to use. Microanalysis were performed by the Analytical Service of the Instituto de Investigaciones Químicas. IR spectra were recorded with Bruker Vector 22 or Tensor 27 spectrometers, and UV-VIS spectra with a Perkin-Elmer Lambda 12 spectrophotometer, using special cuvettes provided with a gastight Young® Teflon valve. NMR spectra were recorded with Bruker 300 and 400 MHz spectrometers. Chemical shifts are expressed relative to TMS. The  $^1\text{H}$  NMR residual resonance of the solvent was used as internal standard and an external reference of  $\text{CF}_3\text{CO}_2\text{H}$  was used for the  $^{19}\text{F}$  spectra of **5**. Magnetic susceptibility measurements were made with a Sherwood Scientific balance model MSB-auto. Magnetic moments are reported at room temperature (298 K) and have been corrected for diamagnetic contributions estimated from Pascal constants.<sup>[19]</sup> Complex **1** was prepared as described in Ref. 6. Pentafluorophenol, hydrogen chloride (1.1 M solution in ether), trifluoroacetic acid and triflic acid were purchased from Aldrich and used as received.

*4.2. General procedure for the reaction of 1 with protic acids in stoichiometric ratio 1:1.* A solution containing approx. 440 mg of compound **1** (0.7 mmol) in 40 ml of THF was stirred at  $-80\text{ }^\circ\text{C}$ , and a second solution containing exactly the equimolar amount of the corresponding acid (HY = perfluorophenol, 0.46 M in hexane; trifluoroacetic acid, 0.88 M in toluene; hydrogen chloride, 1.15 M in diethyl ether; triflic acid, 0.47 M in diethyl ether) was added drop-wise. No colour change was immediately observed, except in the case of triflic acid, which causes the mixture to turn to a reddish hue. The cooling bath was removed and the mixture was allowed to warm slowly. With the rest of the acid reagents (perfluorophenol, hydrogen chloride and trifluoroacetic acid), colour changes were observed only when the temperature rises to ca.  $0\text{ }^\circ\text{C}$ . After stirring the mixture for 1 h at room temperature, 40 ml of hexane were added. This caused the precipitation of the product, which was isolated by filtration and dried in vacuum. The remaining solution was taken to dryness, extracted with hexane (ca. 40 ml) and filtered. The resulting extract has the characteristic purple colour of **1**, and after concentration and cooling to  $-20\text{ }^\circ\text{C}$ , a small amount of crystals of this compound can be recovered. The solids were dried under vacuum, affording crude yields of products **2** – **5** that were below 50 % of the initial amount of **1**.



4.3. *General procedure for the reaction of 1 with protic acids in stoichiometric ratio 1:2.* This is the same procedure described above, but double amounts of the HY reagents were used. After precipitation with hexane the products were filtrated leaving a nearly colourless solution, which evinces total consumption of **1**. The solids were dried under vacuum and recrystallized as indicated below.

4.4. *Complex 2:* Green crystals. Recrystallized from cold THF (-20 °C), Isolated yield, 61 % (0.46 mmol from 0.75 mmol of **1**).  $^1\text{H}$  NMR ( $\text{C}_6\text{D}_6$ , 298 K, 300 MHz),  $\delta$  (ppm): -22.6 ( $\Delta\nu_{1/2} = 53$ , 6H,  $\text{CH}_3\text{-C=N}_{\text{Ar}}$ ); 9.8 ( $\Delta\nu_{1/2} = 107$  Hz, 12 H, *o*- $\text{CH}_3$  Aryl); 12.7 ( $\Delta\nu_{1/2} = 15$ , 4H, *m*-CH Aryl); 17.7 ( $\Delta\nu_{1/2} = 8$ , 6H, *p*- $\text{CH}_3$  Aryl); 34.8 ( $\Delta\nu_{1/2} = 27$ , 1H,  $\text{H}_{4\text{py}}$ ); 72.2 ( $\Delta\nu_{1/2} = 40$ , 2H,  $\text{H}_{3\text{py}}$ ). UV-Vis ( $\text{CH}_2\text{Cl}_2$ ,  $\text{C} = 10^{-4}\text{M}$ ):  $\lambda_{(\text{max})} = 295$  nm ( $\epsilon = 8200$ ); 350 nm ( $\epsilon = 2600$ ), 476 nm ( $\epsilon = 950$ ), 515 nm ( $\epsilon = 1000$ ), 580 nm (shoulder,  $\epsilon = 830$ ). IR (Nujol mull): 1641, 1569  $\nu(\text{C=N})$ ,  $\nu(\text{C=C py})$  1259, 1214  $\nu(\text{C}_{\text{ar}}\text{-O})$ ; 1014, 995  $\nu(\text{C-F})$ .  $\mu_{\text{eff}}$  (magnetic balance): 5.5  $\mu_{\text{B}}$ . Anal. Calc. for  $\text{C}_{39}\text{H}_{31}\text{F}_{10}\text{FeN}_3\text{O}_2$ : C 57.16, H 3.81, N 5.13. Found: C 56.70, H 3.95, N 5.03.

4.5. *Complex 3:* Burgundy-red solid. Recrystallized from  $\text{CH}_2\text{Cl}_2$ . Isolated yield, 40 % (0.26 mmol from 0.65 mmol of **1**).  $^1\text{H}$  NMR ( $\text{CD}_2\text{Cl}_2$ , 298 K, 300 MHz),  $\delta$  (ppm): -11.2 ( $\Delta\nu_{1/2} = 49$  Hz, 1 H,  $\text{H}_{4\text{py}}$ ); 4.1 ( $\Delta\nu_{1/2} = 62$  Hz, 6 H,  $\text{CH}_3\text{-C=N}_{\text{Ar}}$ ); 13.8 ( $\Delta\nu_{1/2} = 107$  Hz, 12 H, *o*- $\text{CH}_3$  Aryl); 15.1 ( $\Delta\nu_{1/2} = 23$  Hz, 4 H, *m*-CH Aryl); 19.2 ( $\Delta\nu_{1/2} = 19$  Hz, 6 H, *p*- $\text{CH}_3$  Aryl); 84.6 ( $\Delta\nu_{1/2} = 49$  Hz, 2 H,  $\text{H}_{3\text{py}}$ ).  $\mu_{\text{eff}}$  (magnetic balance): 5.13  $\mu_{\text{B}}$ . UV-Vis ( $\text{CH}_2\text{Cl}_2$ ,  $\text{C} = 10^{-4}\text{M}$ ): 295 nm ( $\epsilon = 5500$ ); 350 nm (shoulder,  $\epsilon = 2500$ ), 625 nm ( $\epsilon = 540$ ). IR (Nujol mull): 1697  $\nu_{\text{s}}(\text{CO}_2)$ , 1635  $\nu(\text{C=N})$ , 1588  $\nu(\text{C=C py})$ , 1260  $\nu_{\text{as}}(\text{CO}_2)$ , 1202  $\nu(\text{C-F})$ . Anal. Calcd. for  $\text{C}_{32}\text{H}_{33}\text{Cl}_2\text{F}_6\text{FeN}_3\text{O}_4$ : C 54.80, H 4.60, N 6.18. Found: C 54.56, H 4.67, N 5.54.

4.6. *Complex 4.*<sup>[3]</sup> Dark blue solid. Washed with 40 ml of hexane and dried under vacuum. Isolated yield, 53 % (0.34 mmol from 0.65 mmol of **1**).  $^1\text{H}$  NMR ( $\text{CD}_2\text{Cl}_2$ , 298 K, 300 MHz),  $\delta$  (ppm): -22.2 ( $\Delta\nu_{1/2} = 86$  Hz, 6 H,  $\text{CH}_3\text{-C=N}_{\text{Ar}}$ ); 12.5 ( $\Delta\nu_{1/2} = 179$  Hz, 12 H, *o*- $\text{CH}_3$  Aryl); 15.5 ( $\Delta\nu_{1/2} = 73$  Hz, 4 H, *m*-CH Aryl); 21.7 ( $\Delta\nu_{1/2} = 66$  Hz, 6 H, *p*- $\text{CH}_3$  Aryl); 35.5 ( $\Delta\nu_{1/2} = 84$  Hz, 1 H,  $\text{H}_{4\text{py}}$ ); 82.2 ( $\Delta\nu_{1/2} = 94$  Hz, 2 H,  $\text{H}_{3\text{py}}$ ). UV-Vis. ( $\text{CH}_2\text{Cl}_2$ ,  $\text{C} = 10^{-4}\text{M}$ ): UV-VIS ( $\text{CH}_2\text{Cl}_2$   $\text{C} = 10^{-4}\text{M}$ ): 285 nm ( $\epsilon = 7700$ ), 325 nm (shoulder,  $\epsilon = 4700$ ), 675 nm ( $\epsilon = 331$ ). IR (Nujol mull): 1620  $\nu(\text{C=N})$ , 1587  $\nu(\text{C=C py})$ .

4.7. *Complex 5.* Magenta crystals. Recrystallized from cold  $\text{CH}_2\text{Cl}_2$ . Isolated yield, 57 % (0.30 mmol from 0.52 mmol of **1**).  $^1\text{H}$  NMR ( $\text{CD}_2\text{Cl}_2$ , 298 K, 300 MHz),  $\delta$  (ppm): -3.6 ( $\Delta\nu_{1/2} = 52$  Hz, 6 H,  $\text{CH}_3\text{-C=N}_{\text{Ar}}$ ); 0.8 ( $\Delta\nu_{1/2} = 133$  Hz, 12 H, *o*- $\text{CH}_3$  Aryl); 11.6 ( $\Delta\nu_{1/2} = 24$  Hz, 4 H, *m*-CH Aryl); 20.3 ( $\Delta\nu_{1/2} = 11$  Hz, 6 H, *p*- $\text{CH}_3$  Aryl); 22.3 ( $\Delta\nu_{1/2} = 63$  Hz, 1 H,  $\text{H}_{4\text{py}}$ ); 78.7 ( $\Delta\nu_{1/2} = 69$  Hz,  $\text{H}_{3\text{py}}$ ).  $^{19}\text{F}$  NMR ( $\text{CD}_2\text{Cl}_2$ , 298 K, 376 MHz): -14.6 ( $\Delta\nu_{1/2} = 965$  Hz).  $^{19}\text{F}$  NMR (MeCN, 298 K, 376 MHz): -71.0 ( $\Delta\nu_{1/2} = 877$  Hz). UV-Vis( $\text{CH}_2\text{Cl}_2$ ,  $\text{C} = 10^{-4}\text{M}$ ):

$\lambda_{(\max)} = 299 \text{ nm}$  ( $\epsilon = 5500$ );  $355 \text{ nm}$  (shoulder,  $\epsilon = 1800$ );  $550 \text{ nm}$  ( $\epsilon = 820$ ).  $\mu_{\text{eff}}$ :  $4.9 \mu_{\text{B}}$  (magnetic balance,  $25^\circ\text{C}$ ). IR (Nujol mull):  $3345 \nu(\text{OH})$ ,  $1638$ ,  $1619 \nu(\text{C}=\text{N})$ ,  $1588 \nu(\text{C}=\text{C py})$ ,  $1304$ ,  $1214$ ,  $1165 \nu(\text{C}-\text{F})$ . Anal. Calcd. for  $\text{C}_{29}\text{H}_{33}\text{F}_6\text{FeN}_3\text{O}_7\text{S}_2 \cdot 0.5\text{CH}_2\text{Cl}_2$ : C 43.64, H 4.22, N 5.17. Found, C 43.55, H 4.084, N, 5.36.

**4.8. X-ray crystal structure analyses of 2 and 5.** A summary of the crystallographic data and the structure refinement is reported in Table 2. Crystals coated with dry perfluoropolyether were mounted on a glass fiber and fixed under a cold nitrogen stream. The Intensity data were collected on a Bruker-Nonius X8ApexII CCD area detector diffractometer using Mo- $K\alpha$  radiation source ( $\lambda = 0.71073 \text{ \AA}$ ) and graphite monochromator. The data collection strategy used was  $\phi$  and  $\omega$  rotations with narrow frames. Instrument and crystal stability were evaluated from the measurement of equivalent reflections at different measuring times and no decay was observed. The data were reduced using SAINT<sup>[20]</sup> and corrected for Lorentz and polarisation effects, and a semiempirical absorption correction was applied using SADABS.<sup>[21]</sup> The structures were solved by direct methods using SIR-2002<sup>[22]</sup> and refined against all  $F^2$  data by full-matrix least-squares techniques using SHELXTL-6.12<sup>[23]</sup> minimizing  $w[F_o^2 - F_c^2]^2$ . All the non-hydrogen atoms were refined with anisotropic displacement parameters. The hydrogen atoms of compounds 2-5 were included from calculated positions and allowed to ride on the attached atoms with isotropic temperature factors ( $U_{\text{iso}}$  values) fixed at 1.2 times (1.5 times for methyl groups) those  $U_{\text{eq}}$  values of the corresponding attached atoms. Complete structural data have been deposited with CCDC Reference Nos. 964359 (**2**) and 964360 (**5**).

Table 2. Crystallographic data collection, intensity measurements and structure refinement parameters for **2** and **5**.

	<b>2</b>	<b>5</b>
formula	$\text{C}_{39}\text{H}_{31}\text{F}_{10}\text{FeN}_3\text{O}_2 \cdot 2(\text{C}_4\text{H}_8\text{O})$	$\text{C}_{29}\text{H}_{33}\text{F}_6\text{FeN}_3\text{O}_7\text{S}_2$
fw	963.73	769.55
crystal system	Orthorhombic	Monoclinic
space group	<i>Pnma</i>	<i>P2<sub>1</sub>/n</i>
a, $\text{\AA}$	15.7849(5)	15.0793(6)
b, $\text{\AA}$	19.3433(6)	8.8111(4)
c, $\text{\AA}$	14.5566(5)	25.3883(11)
$\alpha$ , deg.	90.00	90.00
$\beta$ , deg.	90.00	102.926(2)
$\gamma$ , deg.	90.00	90.00
V, $\text{\AA}^3$	4444.6(2)	3287.7(2)
Temperature, K	100(2)	100(2)
Z, F(000)	4, 1992	4, 1584
$D_{\text{calc}}$ , $\text{Mgm}^{-3}$	1.440	1.555
$\mu$ , $\text{mm}^{-1}$	0.429	0.670
$\theta_{\text{max}}$ , deg	30.5	30.6
no. reflns collected	106012	86096
no.reflns used	6976	10003

no. of param.	343	441
$R_1(F)$ [ $F^2 > 2\sigma(F^2)$ ] <sup>[a]</sup>	0.0394	0.0540
$wR_2(F^2)$ <sup>[b]</sup> (all data)	0.1151	0.1592
$S$ <sup>[c]</sup> (all data)	1.071	1.062

<sup>[a]</sup>  $R_1(F) = \sum(|F_o| - |F_c|) / \sum|F_o|$  for the observed reflections [ $F^2 > 2\sigma(F^2)$ ].

<sup>[b]</sup>  $wR_2(F^2) = \{\sum [w(F_o^2 - F_c^2)^2] / \sum w(F_o^2)^2\}^{1/2}$ . <sup>[c]</sup>  $S = \{\sum [w(F_o^2 - F_c^2)^2] / (n-p)\}^{1/2}$ ,  
(n = number of reflections, p = number of parameters).

## Acknowledgements

This work was supported by the Government of Spain (project number CTQ2012-30962), the Junta de Andalucía (project number FQM5074) and the European Union (EU) (FEDER funds). MAC thanks CSIC for a predoctoral research fellowship (I3P program).

## References

- [1] a) L. Li, P. T. Gomes, in *Olefin Upgrading Catalysis with Nitrogen-based Metal Complexes, State of the Art and Perspectives., Vol. II* (Eds.: G. Giambastiani, J. Cámpora), Springer, Dordrecht, **2011**, pp. 77-198. b) C. Bianchini, G. Giambastiani, I. Guerrero Rios, G. Montovani, A. Meli, A. M. Segarra, *Coord. Chem. Rev.* **2007**, *250*, 1391-1418.
- [2] M. W. Bouwkamp, E. Lobkovsky, P. J. Chirik, *J. Am. Chem. Soc.* **2005**, *127*, 9660-9661.
- [3] G. J. P. Britovsek, M. Bruce, V. C. Gibson, B. S. Kimberley, P. J. Maddox, S. Mastroianni, S. J. McTavish, C. Redshaw, S. G., S. Strömberg, A. J. P. White, D. J. Williams, *J. Am. Chem. Soc.* **1999**, *121*, 8728-8740.
- [4] a) K. P. Bryliakov, N. V. Semikolenova, V. A. Zakharov, K. P. Talsi, *Organometallics* **2004**, *23*, 5375-5378. B) K. P. Bryliakov, E. P. Talsi, N. V. Semikolenova, V. A. Zakharov, *Organometallics* **2009**, *28*, 3225-3232.
- [5] a) M. Bochmann, *J. Organomet. Chem.* **2004**, *689*, 3982-3998. b) M. Bochmann, *Organometallics* **2010**, *29*, 4711-4740.
- [6] J. Cámpora, A. M. Naz, P. Palma, E. Álvarez, *Organometallics* **2006**, *24*, 4878-4881.
- [7] pK<sub>a</sub> values in water. Note that the acid strength of HY is inversely related to the basicity of Y ligands, which correlates with their ability to donate electron density to the metal centre. Aqueous pK<sub>a</sub> were selected because they are available for the four acids used in this work, but note that the acid strengths of HOTf, HCl, acetic acid and phenol holds in water, acetonitrile and dichloroethane, see ref. [8a].

- [8] a) E. Raamat, K. Kaupmees, G. Ovsjannikov, A. Tummal, A. Kütt, J. Saame, I. Koppel, I. Kaljurand, L. Lipping, T. Rodima, V. Pihl, I. A. Koppel, I. Leito, *J. Phys. Org. Chem.* **2013**, *26*, 162-170. b) J.F.J. Dippy, S.R.C. Hughes, A. Rozanski, *J. Chem. Soc.* **1959**, 2492 - 2498. c) D. Stefanidis, S. Cho, S. Dhe - Paganon, W. P. Jenks, *J. Am. Chem. Soc.* **1993**, *115*, 1650 – 1656.
- [9] I. Fernández, R. J. Trovitch, E. Lobkovsky, P. J. Chirik, *Organometallics* **2008**, *27*, 109-118.
- [10] R. J. Trovitch, E. Lobkovsky, M. W. Bouwkamp, P. J. Chirik, *J. Am. Chem. Soc.* **2009**, *27*, 6264-6278.
- [11] W. A. Addison, T. N. Rao, J. Reedijk, J. van Rijn, G. C. Verschoor, *J. Chem. Soc., Dalton Trans.* **1984**, 1349 – 1356.
- [12] G. J. P. Britovsek, J. England, S. K. Spitzmesser, A. J. P. White, D. J. Williams, *Dalton Trans.* **2005**, 945-955.
- [13] Y. M. Baidei, M. A. Siegler, D. P. Goldberg, *J. Am. Chem. Soc.* **2011**, *133*, 1274-1277.
- [14] F. A. Cotton, G. Wilkinson, C. A. Murillo, M. Bochmann, *Advanced Inorganic Chemistry*, 6th ed., John Wiley & Sons, New York, **1999**.
- [15] K. L. Tokarev, M. A. Kiskin, A. A. Sidorov, G. G. Aleksandrov, V. N. Ikorskii, I. P. Suzdalev, V. N. Novotortsev, I. L. Eremenko, *Russ. Chem. Bull.* **2008**, *57*, 1209-1214.
- [16] D. Lee, S. J. Lippard, *Inorg. Chim. Acta* **2002**, *341*, 1-11.
- [17] a) R. C. Mehrotra, R. Bohra, *Metal Carboxylates*, Academic Press, London, **1983**. B) A. Behr, R. He, K. D. Juszak, C. Krüger, Y. H. Tsay, *Chem. Ber.* **1986**, *119*, 991-1015. c) E. Nakamoto, *Infrared Spectra of Inorganic and Coordination Compounds*, 4th ed., John Wiley & Sons, New York, **1986**.
- [18] G. J. P. Britovsek, V. C. Gibson, S. K. Spitzmesser, K. P. Tellmann, A. J. P. White, D. J. Williams, *J. Chem. Soc. Dalton Trans.* **2002**, 1159-1171.
- [19] G. A. Bain, J. F. Berry, *J. Chem. Ed.* **2008**, *85*, 532-536.
- [20] SAINT, APEX2 Suite, v. 2.1. Bruker AXS Inc., Madison, Wisconsin, USA, **2006**.
- [21] G. Sheldrick, SADABS, APEX2 Suite, v. 2.1. Bruker AXS, Inc., Madison, Wisconsin, USA, **2006**.
- [22] SIR-2002, APEX2 Suite, v., 2.1, Bruker AXS Inc., Madison, Wisconsin, USA, **2006**.
- [23] SHELXTL, v. 6.14. Bruker AXS Inc., Madison, Wisconsin, USA, **2000-2003**.